Applied Soft Computing 34 (2015) 389–401

Contents lists available at ScienceDirect

Applied Soft Computing

journal homepage: www.elsevier.com/locate/asoc

Color image segmentation based on multiobjective artificial bee colony optimization

Tahir Sağ[a], Mehmet Çunkaş[b,*]

[a] Dept of Computer Engineering, Faculty of Technology, Selcuk University, Turkey
[b] Department of Electrical & Electronics Engineering, Faculty of Technology, Selcuk University, Turkey

ARTICLE INFO

Article history:
Received 7 February 2015
Received in revised form 27 April 2015
Accepted 8 May 2015
Available online 22 May 2015

Keywords:
Color image segmentation
Multiobjective optimization
Artificial bee colony
Fuzzy c-means

ABSTRACT

This paper presents a new color image segmentation method based on a multiobjective optimization algorithm, named improved bee colony algorithm for multi-objective optimization (IBMO). Segmentation is posed as a clustering problem through grouping image features in this approach, which combines IBMO with seeded region growing (SRG). Since feature extraction has a crucial role for image segmentation, the presented method is firstly focused on this manner. The main features of an image: color, texture and gradient magnitudes are measured by using the local homogeneity, Gabor filter and color spaces. Then SRG utilizes the extracted feature vector to classify the pixels spatially. It starts running from centroid points called as seeds. IBMO determines the coordinates of the seed points and similarity difference of each region by optimizing a set of cluster validity indices simultaneously in order to improve the quality of segmentation. Finally, segmentation is completed by merging small and similar regions. The proposed method was applied on several natural images obtained from Berkeley segmentation database. The robustness of the proposed ideas was showed by comparison of hand-labeled and experimentally obtained segmentation results. Besides, it has been seen that the obtained segmentation results have better values than the ones obtained from fuzzy c-means which is one of the most popular methods used in image segmentation, non-dominated sorting genetic algorithm II which is a state-of-the-art algorithm, and non-dominated sorted PSO which is an adapted algorithm of PSO for multi-objective optimization.

1. Introduction

Image segmentation is an essential procedure used in low-level preprocessing. Moreover, it is the most important step to analyze images and to extract meaningful data for many applications of computer vision and pattern recognition. This operation partitions a digital image into distinct regions which consist of the pixels with similar attributes such as intensity, color and texture. Great varieties of segmentation techniques have been presented in literature. However, the obtaining segmentation with an exact accuracy is often a very challenging task, especially for natural images. The successes of segmentation algorithms widely depend on the concept of the region homogeneity represented by a similarity criterion and determining the distinctive features extracted from the image. Image segmentation techniques can be categorized into four general approaches: threshold-based, edge-based, region-based, and clustering-based methods [1].

The threshold-based methods assume that an image is composed of regions with different intensity ranges. The optimum threshold values are determined by the histogram of the image which has the valleys between two adjacent peaks. Owing to its simplicity, histogram thresholding is a widely used technique for monochrome image segmentation. But it is not a trivial job for color image because of its multi-dimensional structure [2,3]. The edge-based methods identify the boundaries of objects by applying an edge filter to the image. Unlike the edge-based segmentation which returns boundaries between regions, the region-based methods aim to determine the regions directly. In this technique, segmentation is regarded as spatial clustering. This means that every pixel must be a member of region and the pixels in a region are connected to each other by means of pixel neighborhood. These methods have two operations: merging and splitting. In the merging strategy also known as region growing, initially all pixels are assumed to be a distinct segment which should be merged according to a similarity criterion until no segments remain to be merged. In the splitting

* Corresponding author. Tel.: +90 3322233359.
E-mail address: mcunkas@selcuk.edu.tr (M. Çunkaş).

http://dx.doi.org/10.1016/j.asoc.2015.05.016
1568-4946/

strategy, the entire image is assumed as a single segment which should be split until each region satisfies the homogeneity. Considering the segmentation process that aims to group the pixels in an image with respect to some similarity measures, it can basically be handled as a clustering problem. Determination of cluster validation is a widely studied issue. Many algorithms based on clustering such as fuzzy c-means, Expectation Maximization, and genetic algorithms have been used for image segmentation [4,5].

Recent efforts have demonstrated that the hybrid approaches based on swarm intelligence can be used as an effective tool in this field. Omran et al. [6] proposed a dynamic clustering approach based on particle swarm optimization for image segmentation and they tried to automatically determine optimum number of centroids. ACO-based region-growing approach was proposed by Ramos and Almeida [7]. Huang et al. [8] applied this model for partitioning medical images. Ma et al. [9] proposed a fast image segmentation method based on artificial bee colony algorithm to estimate the appropriate threshold values in a continuous grayscale interval. Cinsdikici and Aydın [10] proposed a hybrid approach of matched filter and ant colony optimization algorithm for extraction of blood vessels in ophthalmoscope images. Aydın and Ugur [11] presented a color clustering method based on ant colony optimization for the detection of flower boundaries. Akay [12] put forward the search abilities of PSO and ABC algorithms on multilevel thresholding. Sag and Cunkas [13] applied an ABC-based clustering algorithm to the image segmentation.

As a new trend, multi-objective optimization algorithms have been used in problem formulation for image segmentation. Multiobjective optimization also known as Pareto optimization is an extension of optimization with single objective. This methodology enables to optimize several conflicting objectives simultaneously and it has been successfully applied in several engineering problems such as electromagnetic absorbers design [14], definition of design variables and loading for I-beam [15], etc. The multiobjective optimization algorithms based on metaheuristic techniques are suitable method to deal with natural image segmentation problem which contains multiple objectives such as maximization of inter-region compactness and minimization of intra-region separation. Nakib et al. [16] used a multiobjective optimization algorithm based on the adapted NSGA2 to find the optimal thresholds for test images. On the other hand, Saha and Bandyopadhyay [17] presented a multiobjective clustering approach for MR brain image segmentation. Two cluster validity indices to be optimized were used in simulated annealing based strategy. Then Saha et al. [18] developed a multiobjective differential evolution based on FCM by using similar validity indices. They applied the algorithm to satellite images with the aim pixel classification. Bong and Rajeshwari [19] submitted a comprehensive review of the nature inspired multiobjective optimization techniques used in image segmentation. They have reported that a typical image segmentation procedure involves feature selection, pattern proximity, grouping and cluster validity analysis. Determination of the feature set plays the most decisive role in clustering. Mostly, only intensity values of pixels are insufficient. Multiple features should be extracted for image segmentation in which the regions to be found can involve edge, color and texture information. Withal, inter-pattern similarity which has conflicting objectives such as spatial coherence and feature homogeneity are related to multiple criteria. Considering the previous studies, clustering technique is generally used for pixel classification by ignoring spatial relationship.

Beside abovementioned categorization, color image segmentation has also been an attractive research topic in this field, which still protects its popularity, since color images have more distinctive features than grayscale images. The human eye can recognize thousands of color shades and intensities whereas only two dozen shades of gray are perceived. The objects which cannot be extracted only from intensity can easily be obtained by using color. In this paper, a new color image segmentation algorithm based on the seeded region growing and multiobjective optimization has been proposed. The segmentation is posed as a clustering problem through grouping image features in this approach. First, a feature vector that consists of seven members is constructed by composing color components, texture and homogeneity datum. Then homogeneous regions in an image are segmented by considering spatial coherence through the seeded region growing technique. On the other hand, cluster validation is ensured by IBMO with respect to compactness of inter-region and separation of intra-regions. IBMO is developed by authors in [20] that is a multiobjective extension of artificial bee colony optimization algorithm. IBMO is used here for automatic determination of both the optimal location of cluster centers and similarity threshold values between regions. In order to test the potential of the proposed algorithm, the segmentation results are compared with other three algorithms: non-dominated sorted PSO (NSPSO) [21], non-dominated sorting genetic algorithm 2 (NSGA2) [22] and fuzzy c-means (FCM) [23]. The comparative results of performance metrics show that the adapted version of IBMO is a promising method for color image segmentation.

The rest of the paper is organized as follows. The Section 2 focuses on the basic theory of multi-objective optimization; also ABC and IBMO algorithms are explained in details. Then the feature extraction techniques are described in Section 3. The proposed color image segmentation approach is presented in Section 4. The experimental results and evaluation metrics are explained in Section 5. Finally, a brief conclusion is presented in Section 6.

2. Methods

Image segmentation problems actually have multiple objectives such as minimizing overall deviation, maximizing connectivity, minimizing the features or minimizing the error rate of the classifier, etc. [24]. In this context, image segmentation problem can be handled as a multiobjective optimization problem (MOO). The multiple-objectives approaches used in literature can be categorized in two classes. These are weighted-sum method and Pareto-Optimal approaches. In the weighted sum approach, the best solution which corresponds to the minimum or maximum value of the problem is sought by combining all objectives into a function with a weighted formula. The first class converts a MOO problem into a single-objective problem. This type of optimization may be preferred as a useful tool in case of non-competing objectives. However, many real world optimization problems such as image segmentation contain more than one conflicting objectives to optimize simultaneously. Unlike the aggregating functions, Pareto-based methods enable the consideration of the dominances between objectives apart from obtaining a set of solutions. In this concept, a solution is called as Pareto Optimal or non-dominated solution that are superior to the rest of the solutions but inferior to other solutions in the search space when considering all objectives [25]. The general formulation of the problem can be defined as follows:

$$\begin{aligned} &\text{Maximize/Minimize} && y = f(x) = \{f_1(x), f_2(x), \ldots, f_M(x)\} \\ &\text{Subject to} && g(x) = \{g_1(x), g_2(x), \ldots, g_J(x)\} \le 0 \\ &&& h(x) = \{h_1(x), h_2(x), \ldots, h_K(x)\} = 0 \\ &\text{where} && x = \{x_1, x_2, \ldots, x_N\} \in X \\ &&& y = \{y_1, y_2, \ldots, y_N\} \in Y \end{aligned} \tag{1}$$

where x is set of the decision or feature vectors and X is the parameter space, y is the objective vector, Y is the objective space, $g(x)$ and $h(x)$ is the constraints imposed on the decision variables.

Optimization algorithms based on swarm intelligence are multi-agent, robust and resilient methods, which are inspired by intelligent attributes of swarms. Their main advantages are the simple agents in communication that are capable of solving complex problems. In this study, a new approach named improved bee colony algorithm for multiobjective optimization (IBMO) is applied to image segmentation in accordance with seeded region growing. The handled problem here is to determine the optimal positions of the seed points with the aid of two cluster validity indices used as the objective functions. IBMO is a well-adapted multiobjective version of simple ABC that has been developed by authors [20]. Brief descriptions of ABC and IBMO are addressed in this section.

2.1. Artificial bee colony optimization (ABC)

ABC is a powerful and efficient algorithm based on the intelligence behavior of honeybee swarm [26]. It consists of three phases: employed bee, onlooker bee and scout bee. In the ABC algorithm, a bee in the swarm represents a possible solution and the nectar amount of a food source corresponds to the quality of the associated solution defined as fitness. The more a solution has high fitness, the more possibility of being selected of this solution by onlooker bees. The number of scout bees is controlled by limit parameter. If a solution representing a food source does not improve during a number of trials, then it is abandoned by its employed bee and the employed bee becomes a scout bee. The number of food sources equals to number of employed bees and also number of employed bees equals to number of onlooker bees. All employed bees initially behaves as scout bees and initial swarm composed of employed bees are generated by Eq. (2)

$$x_{ij} = x^j_{min} + rand(0, 1)(x^j_{\max} - x^j_{\min}) \tag{2}$$

where x_i indicates a solution in the population, $i = \{1, 2, \ldots, SN\}$ and SN is the size of population $j = \{1, 2, \ldots, D\}$ and D is the number of parameters (decision variables) in a solution. According to the selected subrange x^j_{min} is the lower bound of jth parameter and x^j_{max} is the upper bound of jth parameter.

After generating the solutions, fitness values of them are calculated by Eq. (3)

$$fit_i = \begin{Bmatrix} 1/(1+f_i) & f_i \geq 0 \\ 1 + abs(f_i) & f_i < 0 \end{Bmatrix} \tag{3}$$

where fit_i is the fitness value of ith solution in the population.

The employed bee determines a food source in the neighborhood of the food source in its memory and it evaluates the quality of new one. If the nectar amount of new source is better than the old source, employed bee will update its memory with new source. The new source in the neighborhood of the current source is determined by Eq. (4):

$$delta = \phi_{ij}(x_{ij} - x_{kj}) \quad \text{and} \quad v_{ij} = x_{ij} + delta \tag{4}$$

where *delta* is the variance value of new parameter. ϕ_{ij} is a random number between [−1,1]. v_i represents new solution, x_k is the neighbor solution selected randomly, $k \in \{1, 2, \ldots, SN\}$. x_{ij} is jth parameter of ith solution represented by current employed bee. j is a random number in the range of [1,D].

After the employed bees have explored the new food sources, they share their information with onlooker bees. Onlooker bees select an employed bee for guidance. For this purpose, roulette wheel is used by depending on the probabilities calculated by Eq. (5).

$$p_i = \frac{fit_i}{\sum_{SN}^{n=1} fit_i} \tag{5}$$

After the onlooker bees select a food source as a guide, the candidate food source is calculated by Eq. (4). Afterwards, the greedy selection process is applied for the onlooker bees. The best solution achieved so far is memorized. ABC uses only one control parameter which is called limit. A food source will not be exploited anymore and it is assumed to be abandoned when limit is exceeded for the source. So it is replaced with randomly produced solution by Eq. (2) [26].

2.2. Improved bee colony algorithm for multi-objective optimization (IBMO)

IBMO consists of the adaptation of ABC to multi-objective optimization by means of non-dominated sorting strategy and principal concepts of Pareto-Optimal such as Pareto-dominancy, crowding distance (CD), external archive (EXA), etc. In addition, an improvement procedure as local search is inserted to algorithm. The flow diagram of the algorithm is depicted as in Fig. 1. IBMO has been applied to several benchmark functions by considering the number of function evaluations, and it has been compared with the state-of-the-art algorithms in literature. The reported results have demonstrated the effectiveness and superiority of the algorithm [20].

The algorithm starts with a diversification technique to generate the initial solutions. In this technique, the ranges of parameters in a solution are divided into equal sized subranges. All subranges have a frequency value and it equals to zero at first. Then a subrange is selected inversely proportional to its frequency count, and the parameter is generated by the Eq. (2) for its selected subrange. Also its frequency count is incremented by one. This process is repeated for each parameters of a new solution to be generated. The more frequency count, the less selection probability of related range or vice versa. So a well-distributed initial swarm (*also known as Foods*) is obtained in the search space.

Fitness values of generated solutions for each objective functions are calculated by Eq. (6).

$$fit_{in} = \begin{Bmatrix} 1/(1+f_{in}) & f_{in} \geq 0 \\ 1 + abs(f_{in}) & f_{in} < 0 \end{Bmatrix} \tag{6}$$

where fit_{in} denotes the fitness of nth objective of ith solution. The obtained fitness vector is used in Pareto dominance. Before the main loop of the algorithm runs, the first Pareto-front is extracted from the current solutions. The main loop consists of three phases (employed, onlooker and scout bee phases) with a local search procedure to promote the convergence to Pareto Front.

In employed bee phase, a distinct neighbor solution for all solutions is randomly selected from foods set and a new solution is generated in the neighboring of the current and selected solutions by Eq. (4). Here, the parameter to be changed is determined in a random way. It is inversely proportional with frequency count to increase the selection probability of all parameters in the solutions like frequency approach used in diversification method.

After generating a new solution, the improvement procedure begins. It can be considered as a local search which uses a greedy selection process based on constrained dominancy between new and current solutions. If new solution dominates in the current, new solution is added to foods list instead of the current. Furthermore, same delta value is added to same parameter as long as new solution dominates the current, or until the number of iteration exceeds the predefined parameter *limit_count*. This process provides an accelerated convergence effect within selected parameter. The pseudo code of the improvement method is shown in Fig. 2.

At the end of the employed bee phase, non-dominated solutions stored in EXA is updated by Foods. However, it gets hard to control of storing new obtained solution in terms of Pareto dominance since

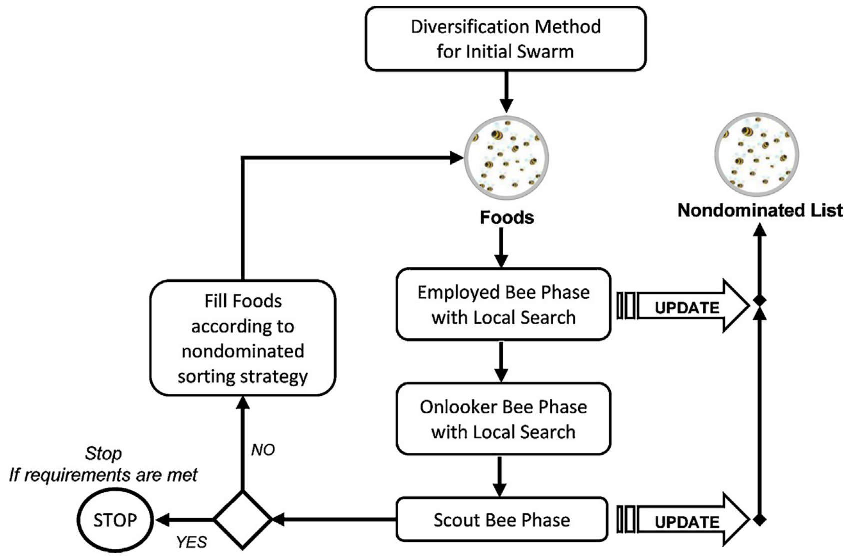

Fig. 1. The flow diagram of IBMO.

the cardinality of EXA extends. Therefore the crowding distance strategy is used to limit the archive size without losing the diversity. The CD of a solution provides the density of solutions surrounding it. It is calculated by summing normalized distance between two nearest solutions on either side of the member along each of the objectives [22]. The solutions are sorted according to each objective separately. Infinite distance is assigned to boundary values for each individual and CD is calculated as follows in Eq. (7).

$$CD(bee_k) = \sum_{k=2}^{n-1} \frac{(bee_{k+1}) \cdot m - (bee_{k-1}) \cdot m}{f_m^{max} - f_m^{min}} \tag{7}$$

where $(bee_{k+1}) \cdot m$ is the value of the mth objective function of the $(k+1)$th solution.

If a new solution is dominated by EXA, it is discarded otherwise it is stored. Also the current solutions dominated by the new solution are removed. When EXA reaches to maximum capacity, the solution with the highest CD value in the archive is removed and new solution is stored.

The next step is the onlooker bee phase. In this phase, onlooker bees take knowledge about the quality of food sources by means of employed bees. Since the best quality solutions obtained so far is stored in EXA, IBMO determines the neighbors from EXA instead of Foods set on the contrary of native ABC algorithm. The roulette wheel method is used and the selection probabilities are applied on a cumulative sum array calculated by CD. In the case of empty external archive, the constraint values of the solutions in the Foods set are used. The determination of parameter to be changed, the generation of new solutions and the improvement procedures are applied similarly to the employed bee phase.

```
if delta equals to zero; Set delta = rand(−0.5, 0.5) otherwise continue
Set newSol = v_i
Set temp = v_i
Set limit_count = 0
REPEAT
    Set limit_count = limit_count + 1
    Set temp_j = temp_j + delta * limit_count
    if temp dominates newSol; break
    Set newSol = temp
UNTIL limit_count < limit
Store newSol into Foods
```

Fig. 2. Pseudocode of improvement method.

Later, the scout bee phase is executed. A trial value is incremented by one whenever related solution fails a greedy selection in both employed and onlooker bee phases. The solutions where trial number exceeds a predefined limit value or an acceptable constraint value do not be improved anymore. Therefore, these solutions are regenerated randomly and related trial values are set to zero. Then the EXA is updated with Foods set as in previous process.

Finally, the current Foods and EXA is combined and sorted according to non-domination level in order to fill the food set for next iteration. To find exactly N solutions, the last front is ordered by means of crowded comparison in descending order, and the less crowded solutions are selected to fill new food set. So elitism of best solution found so far is ensured. The algorithm goes on running again from the employed bee phase until the termination conditions are satisfied such as maximum number of iteration, number of objective function evaluations, error rate, etc.

3. Feature extraction

Feature extraction is a major component of image segmentation, which often consists of boundary detection and texture analysis. In this paper, image segmentation was handled as a clustering problem of similar pixels. Therefore a feature vector that consists of seven elements was extracted. This vector contains color, edge and texture features for each pixels. Firstly, all components of the CIE $L^*a^*b^*$ color space were added to feature vector due to the advantage of defining the relative perceptual differences between any two colors. Then, the pixel texture feature was obtained by means of applying Gabor filter. Finally, local homogeneity was calculated by use of edge and discontinuity of the pixels in HSV color space. These features are discussed below.

3.1. Color spaces of proposed method

Color spaces define the criteria to measure the difference between colors. The criteria play an important role in image analysis and segmentation. The color spaces according to their characteristics can be classified as follows: primary, luminance–chrominance, and perceptual color spaces [27].

RGB color model is quite successful for color display and it comes at the beginning of the primary spaces. However luminance–chrominance and perceptual color spaces have better results comparing to description of the difference and/or similarity between two colors [2].

In this study, HSV perceptual color space is used to calculate local homogeneity values. HSV is frequently preferred in color image analysis and color image segmentation, since HSV can distinguish color information from brightness. Besides, CIE $L^*a^*b^*$ color space is used for Gabor filter. L^* describes brightness, a^* and b^* represent chrominance. LAB colors are absolute due to being exact. Also difference of colors can be calculated by Euclidean distance. Each components of Lab color space is added to feature vector.

3.2. Gabor filter

Gabor filter can be modeled by the response of cells in the primary visual cortex of structure of mammalian eyes through the included parameters. These filters produce a core which allows capturing the continuous color changes in accordance with the sizes used. The first attempt on two-dimensional Gabor wavelet representation is accomplished by Daugman Gabor who gives the name to the method in 1980. Gabor filters have been widely used in pattern analysis applications, since it is thought to be similar to perception in the human visual system.

A two-dimensional Gabor function consists of a sinusoidal plane wave of some frequency and orientation, modulated by a two-dimensional Gaussian function [28]. The two dimensional Gabor filter can be defined as follows [29]:

$$G(x, y, \theta, \lambda, \sigma_x, \sigma_y) = g(x, y, \theta, \sigma_x, \sigma_y).e^{i2\pi\frac{x'}{\lambda}}$$

$$g(x, y, \theta, \sigma_x, \sigma_y) = \frac{1}{2\pi\sigma_x\sigma_y} e^{-\frac{1}{2}\left[\left(\frac{x'}{\sigma_x}\right)^2 + \left(\frac{y'}{\sigma_y}\right)^2\right]} \quad (8)$$

$$x' = x \cos\theta + y \sin\theta$$

$$y' = -x \sin\theta + y \cos\theta$$

where $g(x, y, \theta, \sigma_x, \sigma_y)$ is a two-dimensional Gaussian function, the parameter θ represents the orientation of the normal to the parallel stripes of a Gabor function. λ is the wavelength and $f = 1/\lambda$ is the spatial frequency of the cosine factor. σ_x and σ_y denote the variances in x and y directions, respectively, and it supposed that these are equal here ($\sigma_x = \sigma_y = \sigma$). The ratio σ/λ determines the spatial frequency bandwidth denoted by b.

$$b = \frac{\log_2(\sigma/\lambda)\pi + \sqrt{(\ln 2)/2}}{\log_2(\sigma/\lambda)\pi - \sqrt{(\ln 2)/2}} \quad (9)$$

The filtered image is obtained by processing Gabor filter and two-dimensional convolution operation on an $I(x, y)$ image with $w \times h$ dimensions.

$$GI(x, y, \theta, \lambda, \sigma_x, \sigma_y) = I(x, y) * G(x, y, \theta, \lambda, \sigma_x, \sigma_y) \quad (10)$$

In this study, bandwidth is considered as one. So the standard deviation σ is found by related parameters of bandwidth and frequency. The orientation angle θ is used as recommended in [30]. It is defined as angle $\pi/6$ and its folds ($\theta = \{0, \pi/6, \pi/3, \pi/2, 2\pi/3, 5\pi/6\}$). The frequency values are obtained by Eqs. (11) and (12) as recommended in [30].

$$F_H = 0.25 + 2^{(i-0.5)}/w \quad 0.25 \le F_H < 0.5 \quad (11)$$

$$F_H = 0.25 - 2^{(i-0.5)}/w \quad 0 < F_L < 0.25 \quad (12)$$

where $i = 1, 2, \ldots, \log_2(w/8)$, and w is the width of image.

Gabor filter is applied on the lightness component L of CIE Lab color space in order to extract the texture feature. Because of the fact that the other components a and b are chromaticity components and texture data is generally independent of color, the component L is sufficient. Local median energy of Gabor sub-band coefficients is used in the proposed method as texture feature.

3.3. Local homogeneity

Local homogeneity quantifies the uniformity of a region in the image. It substantially makes use of the local information measured from image. Homogeneity is defined as a composition of standard deviation and discontinuity of color components [31].

The normalized standard deviation of color component of a pixel P_{ij} at the location (i, j) in a $M \times N$ sized image is calculated as follows:

$$V_{ij} = \frac{v_{ij}}{v_{max}} \quad \text{and} \quad v_{ij} = \sqrt{\frac{1}{d^2} \sum_{p=i-((d-1)/2)}^{i+((d-1)/2)} \sum_{q=j-((d-1)/2)}^{j+((d-1)/2)} (P_{ij} - \mu_{ij})^2} \quad (13)$$

where $v_{max} = max\{v_{ij}\}$, $0 \le i, p \le M-1$, $0 \le j, n \le N-1$.

μ_{ij} is the mean of the color component of a pixel P_{ij} within $d \times d$ (such as 5×5) window w_{ij}. HSV color space stands for hue, saturation and value. It is calculated as follows:

$$\mu_{ij} = \frac{1}{d^2} \sum_{p=i-((d-1)/2)}^{i+((d-1)/2)} \sum_{q=j-((d-1)/2)}^{j+((d-1)/2)} P_{ij} \quad (14)$$

The discontinuity of color component is calculated by the magnitude e_{ij} of the gradient at location (i, j). The gradient is obtained by Sobel operator in a $t \times t$ (such as 3×3) window.

$$E_{ij} = \frac{e_{ij}}{e_{max}} \quad \text{and} \quad e_{ij} = \sqrt{{G_x}^2 + {G_y}^2} \quad (15)$$

where $e_{max} = max\{e_{ij}\}$, G_x and G_y are the components of the gradient of color component in the x and y directions, respectively.

The local homogeneity of a pixel P_{ij} is represented as;

$$H_{ij} = 1 - E_{ij} \times V_{ij} \quad (16)$$

The value of the homogeneity at each location of an image has a range from [0,1]. The more uniform the local region surrounding a pixel, the larger the homogeneity value the pixel.

4. Proposed method

The outline of the proposed segmentation method is demonstrated in Fig. 3. This method involves three stages: (1) abovementioned features extraction from color image, (2) determination of the optimal positions of the seed points and optimal similarity values by running IBMO, and (3) seeded region growing procedure.

A feature vector sized NPx7 is formed by the extraction of pixel-level features. The vector involves the components namely; three local homogeneity values for all components of HSV color space, a combined texture feature obtained by Gabor filter, and all three components of CIE Lab color space.

In this method, segmentation process is implemented by a modified seeded region growing (SRG) technique. Region-based techniques group pixels into homogeneous regions. This homogeneity is represented by a similarity criterion. In order to quantify

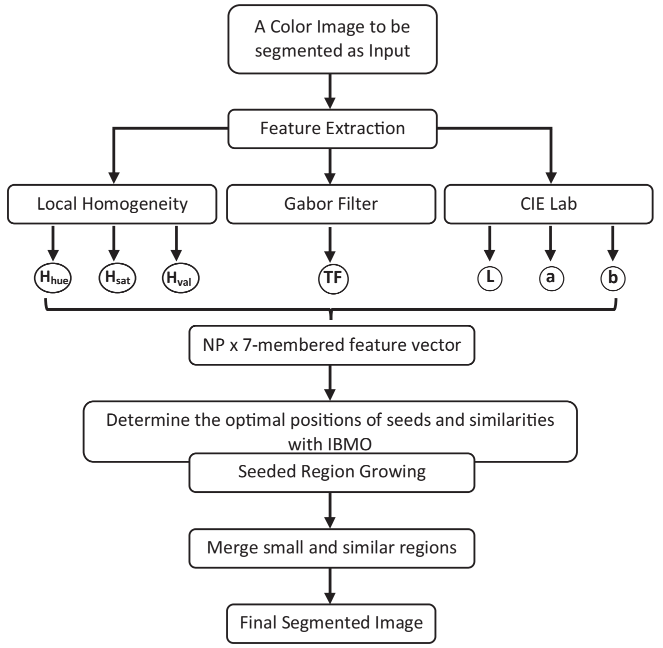

NP: number of pixels in the color image; TF: Texture Feature
H_{hue} - H_{sat} - H_{val} : Local homogeneities of Hue, Saturation, and Value respectively

Fig. 3. Block diagram of the presented method.

the distance or similarity between the pixels, Euclidean distance is calculated by the feature vector as in Eq. (17).

$$dist(p_1, p_2) = \sqrt{\sum_{k=1}^{7} (F(p_1, k) - F(p_2, k))^2} \tag{17}$$

where $dist(p_1, p_2)$ represents the similarity between the pixels p_1 and p_2. $F(n, k)$ is the feature vector of nth pixel of kth feature $\{H_{hue}, H_{sat}, H_{val}, TF, L, a, b\}$.

SRG starts from the initial centroids known as seed points in region growing terminology. Similarity of the adjacent pixels is checked and similar pixels are incorporated to corresponding regions. The pixels are labeled with a symbol of the region they belong to. The seeds are further replaced by the centroids of the generated regions by the additional pixels in each step. All the labeled pixels are called as allocated pixels whereas the unlabeled pixels are called as unallocated pixels. This labeling procedure is repeated until all the pixels in the image have been allocated to the corresponding regions. The success of SRG depends largely on the initial seeds and homogeneity criterion [32].

The SRG method used in this study can be explained in four stages. First, a vector that contains the distances between all seed points and pixels in the image is found. Second, the belonging probabilities of the pixels to all seed points is calculated by membership function of FCM shown in Eq. (18).

$$u_{ij} = \frac{1}{\sum_{C}^{k=1} \left(\frac{x_i - c_j}{x_i - c_k} \right)^2} \tag{18}$$

where u_{ij} is the degree of membership of x_i in the region j, x_i is the ith pixel in the image, c_j is the seed of jth region, and $||*||$ is any norm expressing the similarity between any measured data and the seed point.

Then a binary matrix is created by a convolution mask that filters the obtained probabilities with a threshold value. If the threshold is greater than the probability, matrix value is set to zero; otherwise, it is set to one. Finally, the connected component labeling method

Fig. 4. Representation of a solution in IBMO.

is applied on the binary matrix for the related seed point, and then pixels in the obtained region are labeled. This process is repeated for all seeds and unlabeled pixels, respectively. Thus, regions are segmented faster. At the end of this procedure, unallocated pixels can be remained. These are handled as constraint and assigns to the closest region in the post-processing stage.

In order to achieve a more accurate segmentation result, IBMO provides three important contributions to the proposed SRG based method. These contributions are:

- Assigning the optimal position of seeds (in other words, indices of pixels in the image)
- Determining threshold values for each seed points so that these values are used as the homogeneity criterion by comparing with the distance between a seed and its neighbor pixels.
- The evaluation ability of segmentation quality in considering with multiple criteria as a multi-objective optimization tool.

Each solution x_i ($i = 1, 2, \ldots SN$) in IBMO is a $2 \times D$-dimensional vector. Here, D is the number of seeds and it is set to a value greater than the estimated one by considering the possibility of falling in the same region. The solution x_i can be represented as in Fig. 4. The IBMO generates location index of the seeds in the set of $\{1, 2, \ldots, NP\}$ and threshold values between [0,1] randomly. The parameter $NP = I_{width} \times I_{height}$ is the number of pixels in an image.

Considering the image segmentation is a spatial clustering of similar pixels in an image, two criteria have been widely considered to be sufficient to assess the quality of clustering [33]. These are compactness and separation. The aim of the clustering procedure is to provide the maximum compactness and minimum separation which means the intra-cluster similarities and inter-cluster similarities, respectively. In this context, the process of measuring how well the image segments contain true pixels can be considered as cluster validation. There are several cluster validity indices. Some of the well-known cluster validity indices in literature are Dunn, Davies-Bouldin, Silhouette, S_Dbw, CS, Sym, Turi, etc. [34,35]. Some of them are computationally expensive. Most of them combine the cluster compactness and separation into a quality function. It is performed by a division or a summing operation although these two criteria are often conflicting objectives.

At this point, IBMO is integrated to the proposed method with the aim of evaluating compactness and separation as the distinct objective functions. In addition, any two or more validity indices which are suitable for dataset can be used together. S_Dbw validity index [35] is selected here. It is formulated as follows in Eq. (19):

$$S\_Dbw = scat(NC) + Dens\_bw(NC) \tag{19}$$

It consists of summing the terms of scattering and density. The scattering measures the compactness of the clusters and it is defined as;

$$Objective1 = scat(NC) = \frac{1}{NC} \sum_{k=1}^{NC} \frac{||\sigma(c_k)||}{||\sigma(S)||} \tag{20}$$

where $\sigma(c_k)$ is the variance of cluster c_k and $\sigma(S)$ is the variance of the dataset S. The density term measures the separation of clusters

	1	2	3	4	5	6	7	8
1	1	1	1	1	2	2	2	2
2	1	1	1	1	2	2	2	2
3	1	1	1	1	2	2	2	2
4	1	1	1	1	2	2	2	2
5	2	2	2	2	2	2	2	2
6	2	2	2	2	2	2	2	2
7	2	2	2	2	2	3	3	3
8	2	2	2	2	2	3	3	3

S_1

	1	2	3	4	5	6	7	8
1	1	1	1	1	2	2	2	2
2	1	1	1	1	2	2	2	2
3	1	1	1	2	2	2	2	2
4	2	2	2	2	2	2	2	2
5	2	2	2	2	2	2	2	2
6	2	2	2	2	3	3	3	3
7	2	2	2	2	3	3	3	3
8	2	2	2	2	3	3	3	3

S_2

	1	2	3
1	11	5	0
2	0	36	3
3	0	0	9

M

Fig. 5. Illustration of confusion matrix for segmentations S1 and S2.

and it is defined as;

$$Objective2 = Dens_{bw(K)} = \frac{1}{NC(NC-1)} \sum_{k=1}^{NC} \sum_{l=1 \backslash l \neq k}^{NC} \frac{density(c_k, c_l)}{max\{density(c_k), density(c_l)\}} \tag{21}$$

where $density(c_k) = \sum_{s_i \in C_k} f(s_i, \bar{c}_k)$; $density(c_k, c_l) = \sum_{s_i \in C_k \cup C_l} f\left(s_i, \frac{\bar{c}_k + \bar{c}_l}{2}\right)$; $f(s, c_k) = \begin{cases} 0 & \text{if } density(s_i, c_k) > stdev(C) \\ 1 & \text{otherwise.} \end{cases}$;
$stdev(C) = 1/NC \sqrt{\sum_{c_k \in C} \sigma(c_k)}$

Instead of the combination, IBMO uses S_Dbw index as two objective functions in order to measure the fitness of a solution which contains the centroids of regions and similarity threshold values.

The unlabeled pixels in the image are handled as constraint of optimization problem. At end of an evaluation of all seed points, the ratio of number of unlabeled pixels to the total number of pixels in the image is calculated. If this is lower than 0.25, it is ignored to complete in the post-processing stage. Otherwise it is assigned to constraint value for constrained-Pareto dominance. Thus, selection pressure is increased so as to address much more pixels.

Finally a post-processing is applied to the pre-segmented image. In this step, a closing operation is firstly applied to eliminate small areas. Then region growing procedure is repeated for unlabeled pixels until all pixels belong to a region. Small regions which are smaller than predefined region size are merged the nearest region by co-occurrence matrix. The standard deviations of obtained regions in previous steps are calculated. The highest value is selected as threshold for unlabeled pixels.

5. Results and performance evaluation

The evaluation of image segmentation is generally a difficult task because of its subjective nature. So the most common evaluation methods are based on comparing the obtained results with a predetermined hand-labeled set of ground-truth segmentations. In this study, three kinds of consistency errors are used to measure the effectiveness of segmentation. This section consists of three parts. Firstly, evaluation metrics used in this study are explained briefly. Then how the parameters are selected is clarified. Finally, experimental results are discussed in detail.

5.1. Evaluation metrics

Martin et al. [36] presented two error measures based on a definition of local refinement error (LRE). This metric shows a degree of overlapping between segmentation and its human perceptual partitioning. It means that the error should be lower, even zero if one is a refinement of the other. Local Refinement Error is defined as follows:

$$\mathrm{LRE}(S_1, S_2, p_i) = \frac{\left| R(S_1, p_i) \backslash R(S_2, p_i) \right|}{\left| R(S_1, p_i) \right|} \tag{22}$$

where S_1 and S_2 are two segmentations of the same image. $R(S, p_i)$ is the set of pixels corresponding to the region in segmentation S that contains pixel p_i. $\backslash$ denotes the set difference, and $|x|$ is the cardinality of set x.

LRE values of all pixels in the image are quickly computed by using $n \times m$ confusion matrix (M) of two segmentations: S_1 consists of n regions and S_2 consists of m regions. M denotes the area of intersection of regions from S_1 and S_2. An example of confusion matrix calculation is illustrated in Fig. 5. Also pseudo-code of LRE is shown in Fig. 6.

Note that LRE is not symmetric, so summation of all LRE matrix is not sufficient. To rectify this situation in each direction at each pixel, local consistency error (LCE) and global consistency error (CGE) are used. LCE allows refinement in different directions in different parts of the image. LCE is defined as in Eq. (23) where n is the number of pixels in entire image [37].

$$\mathrm{LCE}(S_1, S_2) = \frac{1}{n} \sum_{i=1}^{n} \min\{\mathrm{LRE}(S_1, S_2, p_i), \mathrm{LRE}(S_2, S_1, p_i)\} \tag{23}$$

Global consistency error forces all local refinements to be in the same direction and it is defined as follows:

$$\mathrm{GCE}(S_1, S_2) = \frac{1}{n} \min\left\{ \sum_{i=1}^{n} \mathrm{LRE}(S_1, S_2, p_i), \sum_{i=1}^{n} \mathrm{LRE}(S_2, S_1, p_i) \right\} \tag{24}$$

Both metrics are in the range [0,1] and lower metric values show better segmentation outcomes. To overcome the problem of

```
for i = 1 to n
    region_i = Σ_j M_ij
    for j = 1 to m
        ind= find indices where S1equals i and S2equals j
        LRE(ind) = (region_i − M_ij)/region_i
endfor j
end for I
```

Fig. 6. Pseudo-code of LRE calculation for all pixels – LRE(S_1, S_2).

Table 1
Common control parameters for all algorithms.

Parameter	Value
Maximum evaluations	50
The smallest region size	500
External archive size	10
Unallocated pixel ratio	0.25

degeneration of segmentations, LRE is adapted to a measure that penalizes dissimilarity between segmentations that are proportional to the degree of region overlap. It is known as bidirectional consistency error (BCE) and defined as follows [37]:

$$BCE(S_{test}, \{S_k\}) = \frac{1}{n}\sum_{i=1}^{n}\min_k\{\max\{LRE(S_{test}, S_k, p_i), LRE(S_k, S_{test}, p_i)\}\} \tag{25}$$

where S_{test} is the obtained segmentation and $\{S_k\}$ denotes a set of available ground-truth segmentations of an image. In order to simplify the comparison of segmentations, all of the three region-based approaches are generally defined as an accuracy indices in literature and these can be defined as follows: LCI = 1 − LCE, GCI = 1 − GCE, and BCI = 1 − BCE; nevertheless, natural forms of consistency errors and sum of all are given in this paper.

5.2. Parameter selection

All methods are applied to all test images with size of 240 × 160 for 500 function evaluations. Some control parameters are common for all algorithms such as swarm size (*NP*), external archive size (*EXA*) and the smallest region size. The common control parameter values are given in Table 1. Besides these parameters, forecasting number of regions and determination of limit parameter value are crucial factors for the performance of the algorithms.

In this context, four steps are implemented during the segmentation process. These steps are illustrated in Fig. 7. First of all, IBMO is initialized with a small colony with 20 members. It is run for different number of regions in the set of {2, 3, 4, 5} and for different number of limit values in the set of {0,5,10,15,20}. So 20 distinct pre-runnings are implemented, since combination of parameter values equals to 4 × 5 = 20. These runs consume very little time, because the number of function evaluations is only set to 50 in this step. For instance, this step is done for each test image and the results of pre-runnings for the image 3096 are shown in Table 2. Consistency errors, objective functions' values, elapsed time and number of feasible solutions found in that running are presented in Table 2.

In the second step, the forecasting region number and limit are selected by using the results of pre-runnings. Considering two indicators segmentation quality (*total consistency error*) and cluster validity (*S_Dbw*), the parameters are determined. It can be seen that there are two best running for the image 3096 as can be seen in Table 2.

In the first best running the best total consistency error is 0.099622, number of region is 4 and limit is 5. In the second best running the best S_Dbw value is 0.067871, number of region is 3 and limit is 5. The region number is set to the region number of the running which has higher one between these two runnings. This is a robust forecasting way. Choosing the number of regions as very high or very low slows the convergence. The limit value is set to mean of two runnings. The selected parameters of all test images used in this paper are shown in Table 3.

The third step of flowchart is running of the algorithms for 500 function evaluations. In this step algorithms are executed 10

Fig. 7. Flowchart of the proposed segmentation method.

Table 2
The results of pre-runnings for the image 3096.

Region	Limit	Feasible solution	LCE	GCE	BCE	Total consistency error	Scattering	Density	S_Dbw	Elapsed time (s)
2	0	1	0.034198	0.024060	0.047180	0.105438	0.914569	0.010385	0.924953	1.305310
	5	1	0.033655	0.022781	0.048486	0.104921	0.306425	0.001675	0.308100	0.918317
	10	2	0.040758	0.030900	0.055720	0.127379	0.926912	0.026795	0.953708	1.048002
	15	3	0.033701	0.022547	0.049751	0.105999	0.686253	0.005141	0.691393	4.098121
	20	0								0.953178
3	0	1	0.035481	0.031272	0.038274	0.105028	0.158427	0.243995	0.402422	1.468747
	5	1	0.028786	0.028371	0.303048	0.360205	0.067871	0.000000	0.067871	3.968405
	10	1	0.033771	0.019680	0.060419	0.113869	0.380538	0.233965	0.614503	1.087864
	15	0								1.535403
	20	1	0.030549	0.030129	0.046495	0.107172	0.202062	0.088580	0.290642	1.589586
4	0	0								1.768662
	5	1	0.031508	0.018884	0.049230	0.099622	0.491916	0.544024	1.035941	1.530317
	10	0								1.552668
	15	0								1.412377
	20	0								1.705617
5	0	0								1.827194
	5	0								1.696940
	10	0								1.818752
	15	1	0.033145	0.017487	0.074201	0.124833	0.533543	0.337834	0.871377	2.130782
	20	1	0.030164	0.029318	0.161644	0.221125	0.067158	0.379882	0.447040	2.758318

Colony size = 20.

Table 3
Selected parameters for test images.

	3096	42049	62096	86016	113016	135069	299091
Forecasting region number	4	9	4	2	5	4	3
Limit	5	10	10	15	10	10	10

Table 4
Running results of the proposed segmentation method IBMO on the image 3096 for 500 function evaluations.

	NNS	NRF	LCE	GCE	BCE	Total consistency error	Scattering	Density	S_Dbw	Elapsed time (s)
Running-1	6	2	0.031536	0.022609	0.041679	0.095824	0.369667	0.000000	0.369667	28.146870
Running-2	3	2	0.028850	0.024367	0.029078	0.082295	0.189290	0.211740	0.401030	22.261440
Running-3	5	2	0.033778	0.029902	0.034255	0.097935	0.836958	0.252941	1.089899	17.576708
Running-4	1	2	0.033364	0.019479	0.058516	0.111359	0.304323	0.313017	0.617340	28.537790
Running-5	6	2	0.026904	0.022389	0.026580	0.075873	0.189680	0.452645	0.642325	21.999283
Running-6	4	2	0.029992	0.022558	0.035460	0.088010	0.905638	0.001843	0.907482	18.238793
Running-7	4	2	0.030907	0.024931	0.033433	0.089271	0.348370	0.105275	0.453644	17.896590
Running-8	3	2	0.037470	0.028424	0.049357	0.115250	0.158221	0.247190	0.405410	17.787398
Running-9	4	2	0.029114	0.020498	0.036771	0.086383	0.496398	0.000044	0.496443	21.481115
Running-10	7	2	0.029865	0.026297	0.029680	0.085842	0.484033	0.344284	0.828317	18.518198

NNS, number of non-dominated solutions; NRF, number of regions found.
Colony size = 50.

independent runs for each image. Finally post-processing step is implemented and segmented image is obtained by assigning all pixels to a region. The results of 10 runnings of IBMO on the test image 3096 for 500 function evaluations are shown in Table 4.

5.3. Experimental results

The proposed segmentation method is applied on several test images obtained from the Berkeley segmentation dataset (BSDS) [36]. BSDS is commonly used in literature as a benchmark tool. It provides test images for researchers interested in image segmentation and boundary detection. The segmentation database consists of 300 grayscale and color natural images. Moreover, it contains hand-labeled segmentations of these images illustrated by 30 human subjects. In this paper, segmentation outcomes are evaluated by exploiting the region-based consistency metrics to determine whether the ground-truth and obtained segmentations are consistent. In addition, three benchmarking algorithms are applied to same test images for comparison of segmentation results. The benchmarking algorithms are NSGA2 which is the state-of-the-art multiobjective optimization technique, NSPSO which is a multiobjective particle swarm optimization algorithm proposed

Table 5
Results of evaluation metrics for the proposed method and other benchmarking algorithms.

BSDS test image number	Alg.	LCE	GCE	BCE	Total error	Scattering	Density	S_Dbw	Elapsed time (s)	Mean time (s)
3096	IBMO	0.026904	0.022389	0.026580	0.075873	0.189680	0.452645	0.642325	21.999283	21.244419
	NSPSO	0.029631	0.025557	0.032188	0.087375	0.250551	0.000000	0.250551	31.713330	24.772340
	NSGA2	0.032267	0.031382	0.044001	0.107650	0.017324	0.252256	0.269581	7.951744	224.787879
	FCM	0.035146	0.031644	0.034811	0.101600				4.297040	4.270320
42049	IBMO	0.127600	0.126887	0.315882	0.570370	0.204968	0.748724	0.953692	33.277100	29.966519
	NSPSO	0.129081	0.123707	0.416388	0.669176	0.193324	0.639812	0.833136	30.056306	30.924711
	NSGA2	0.180821	0.163823	0.291493	0.636137	0.000129	0.000000	0.000129	76.098348	59.246045
	FCM	0.377183	0.338840	0.632877	1.348900				18.689864	18.635147
62096	IBMO	0.050142	0.041711	0.052910	0.144763	0.080334	0.000000	0.080334	19.334017	18.580924
	NSPSO	0.068731	0.048576	0.061188	0.178495	0.022984	0.000000	0.022984	21.884963	20.111907
	NSGA2	0.067914	0.054074	0.384713	0.506700	0.000119	0.000000	0.000119	50.745152	62.421526
	FCM	0.102107	0.094006	0.264986	0.461098				10.385511	10.759900
86016	IBMO	0.020326	0.020326	0.273596	0.314249	0.182435	0.502460	0.684896	9.260838	8.257934
	NSPSO	0.023244	0.023244	0.272545	0.319032	0.209643	0.002889	0.212532	9.852829	9.069223
	NSGA2	0.029167	0.029167	0.273544	0.331877	0.123098	0.000000	0.123098	33.468635	236.781059
	FCM	0.048687	0.048686	0.296424	0.393797				4.271056	4.257568
113016	IBMO	0.090185	0.088903	0.183136	0.362224	0.204651	0.020822	0.225473	17.257824	16.756211
	NSPSO	0.096012	0.095509	0.191842	0.383363	0.192109	0.020362	0.212472	15.285761	16.801116
	NSGA2	0.152569	0.115728	0.291876	0.560174	0.012346	0.000000	0.012346	7.806258	1285.950599
	FCM	0.192610	0.183654	0.519677	0.895942				10.231946	10.431204
135069	IBMO	0.013899	0.013807	0.015201	0.042907	0.354371	0.436605	0.790976	23.437318	29.523659
	NSPSO	0.010745	0.009592	0.029849	0.050186	0.258097	0.000000	0.258097	51.923066	47.590460
	NSGA2	0.050848	0.038165	0.880366	0.969380	0.001322	0.729614	0.730936	314.049001	286.549701
	FCM	0.032415	0.020859	0.637633	0.690908				8.269594	8.252442
299091	IBMO	0.014711	0.014707	0.136737	0.166155	0.214982	0.060953	0.275935	15.233427	14.751328
	NSPSO	0.015828	0.015819	0.139554	0.171201	0.402444	0.002326	0.404770	16.336937	16.601441
	NSGA2	0.076569	0.076569	0.609592	0.762729	0.012849	0.000000	0.012849	4734.349180	4456.687256
	FCM	0.292942	0.140141	0.418282	0.851365				6.379537	6.349791

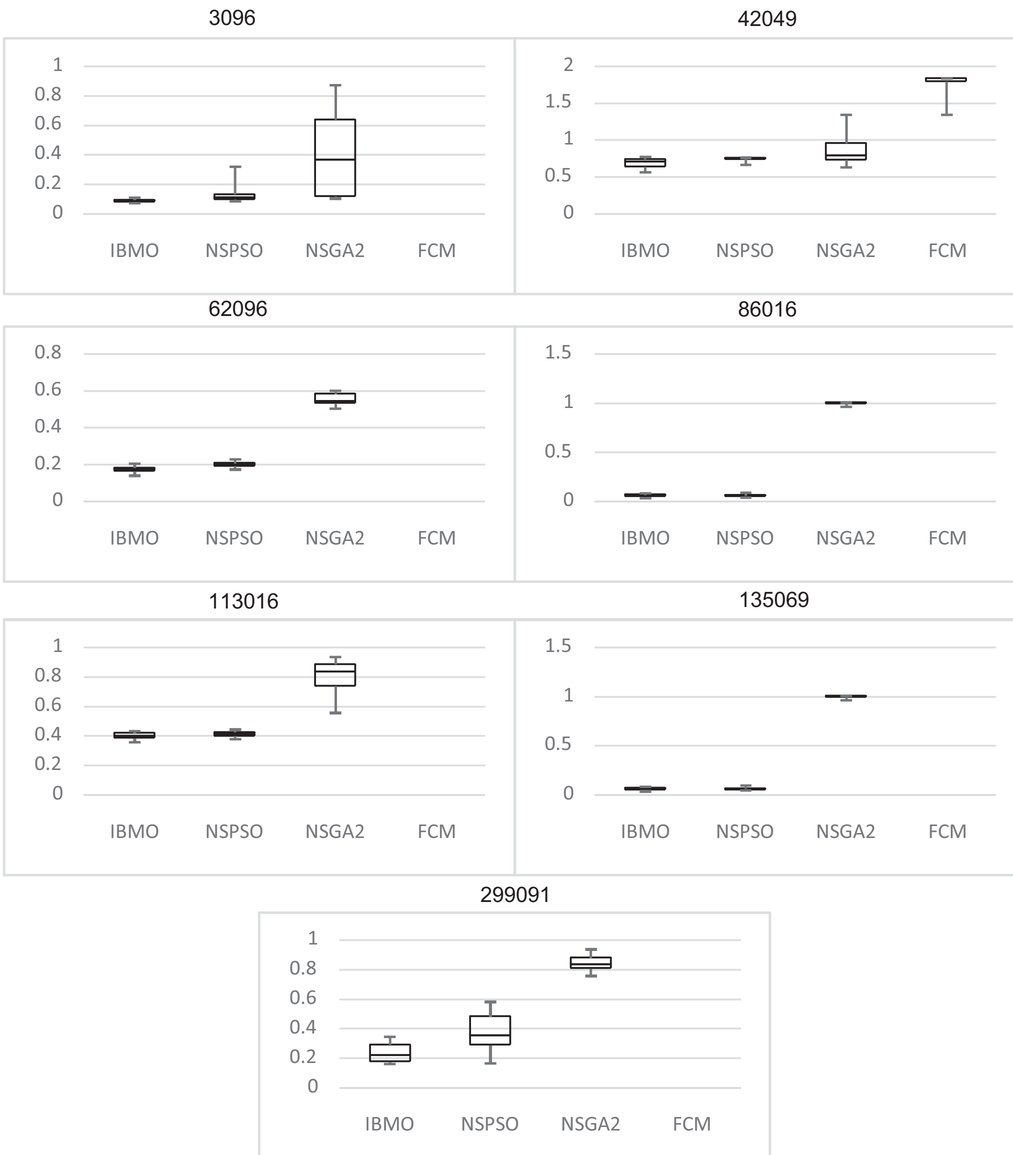

Fig. 8. Box plots for total consistency errors.

for image segmentation [21] and FCM which is one of the most popular clustering methods used in image segmentation. All four algorithms use same feature vectors and common parameter values to segment the images. The three algorithms IBMO, NSPSO and NSGA2 are run to determine seed points and thresholds. Then the same post-processing phase used in proposed approach is applied to images in order to complete unallocated pixels. On the other hand, FCM does not require this process. The forecasting region number and feature vector are sufficient for FCM.

Segmentation results of the proposed method (IBMO) and all other benchmarking algorithms (NSPSO, NSGA2 and FCM) are given in Table 5 which consists of 11 columns. The first two columns show id numbers of test images and algorithm headers. The next three columns show the consistency errors: LCE, GCE and BCE, respectively. Also total consistency error is given in column 6. The calculated values of objective functions (scattering and density) are given in column 7 and 8. Since cluster validity index S_Dbw is an aggregation function of scattering and density, it is given in column 9. These values were obtained before the post-processing phase.

Multiobjective optimization algorithms can produce multiple outcomes as a course of their natures. In this study, the best solution means that it has the lowest total consistency error between multiple solutions. So the selected solution is memorized at the end of a running. The values in Table 5 have been obtained by choosing the best one of 10 runs of algorithms for each image. The elapsed time of the selected best running result and mean time for each algorithm are also presented in column 10 and 11, respectively. The proposed algorithm IBMO and other benchmarking algorithms were implemented in Matlab and all algorithms have been run on a personal computer with a Intel core i7-2600 3.40 GHz CPU, 10 GB memory and Windows operating system.

The best total consistency result for each test images has a gray colored background. It can be seen that the proposed method has a significant accuracy with respect to these region-based consistency indices. Furthermore, the proposed method achieved the best values between all algorithms regarding to the total consistency error. IBMO and NSPSO algorithms achieved good segmentation results with respect to cluster validity and consistency of hand labeled images in an acceptable timing. Although NSPSO has a more stable running characteristic than NSGA2, IBMO gets a little more successful and uniform results for all runs. The uniformity of results generated by the algorithms can be seen in box plot diagrams. For

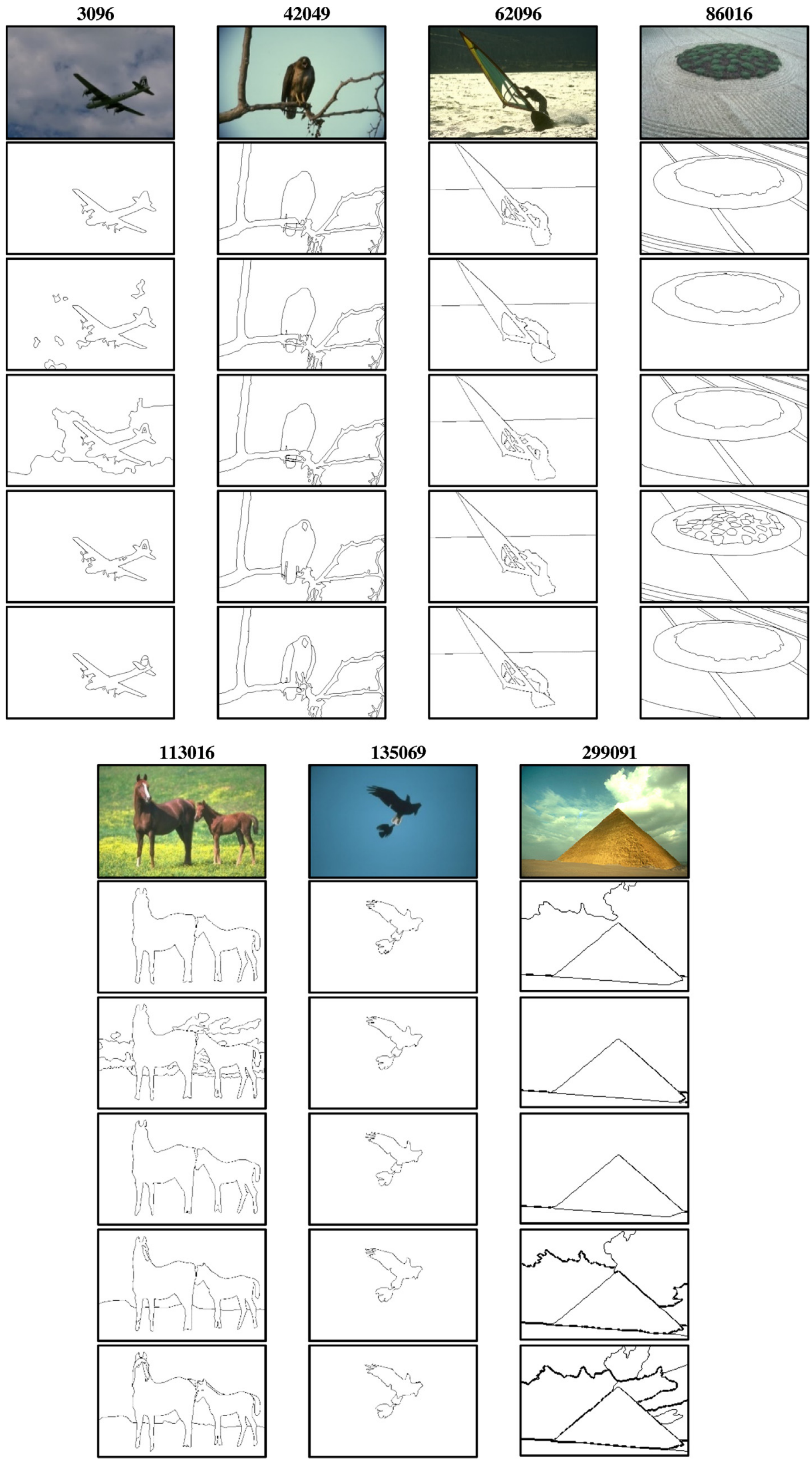

Fig. 9. Hand-labeled segmentations of test images.

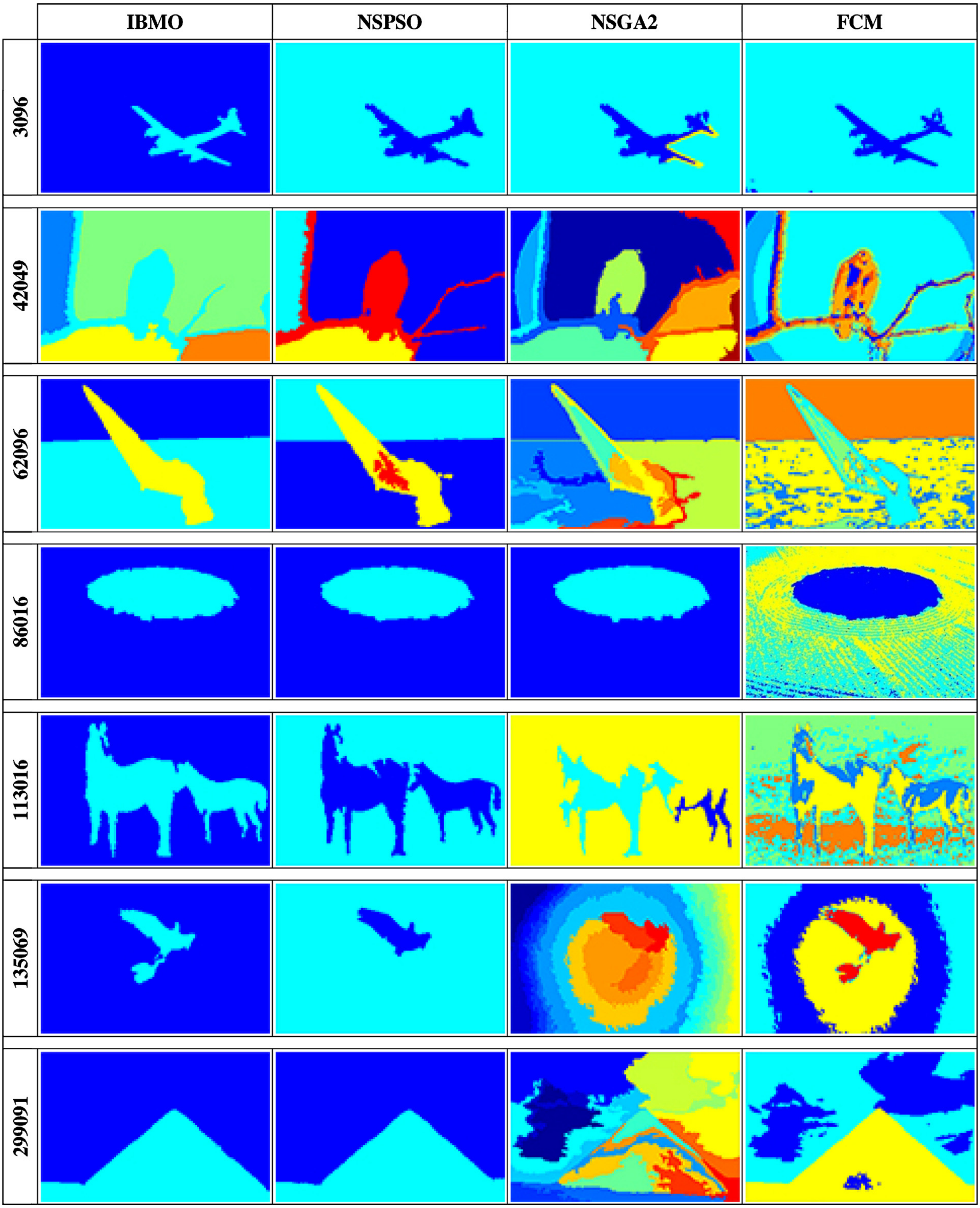

Fig. 10. Comparisons of ground-truths and obtained segmentations.

this purpose, the box plots of total consistency errors for 10 runs are given in Fig. 8. IBMO ensures this stability owing to its local search procedure. On the other hand, NSGA2 consumes too much times for satisfying the constraint function. It could not find any non-dominated solution in some runs. FCM is not a population-based method unlike the other benchmarking algorithms. So FCM is a fast clustering technique that guarantees the uniformity. But it has an important disadvantage as related to spatial connectivity of the pixels in a region. In BCE evaluation, five different human-labeled segmentations are used for all images. The ground-truths of images are given in Fig. 9. LCE and GCE use the segmentations in the first row. All human-labeled segmentations for each test image have been used to calculate BCE as given in Table 5. Also Fig. 10 illustrates the comparison results for the proposed method and other algorithms. As shown in figures, results of the proposed method are promising in particularly for image segmentation applications.

6. Conclusion

In this paper, a new segmentation algorithm has been proposed for color images. Segmentation is posed as a multiobjective clustering problem realized through grouping image features which have a decisive role to obtain the regions of interest. Some of major features for natural images are extracted by local homogeneity and Gabor filter. The proposed method is based on multiobjective optimization (IBMO) and seeded region growing technique. IBMO provides three important contributions to the proposed seeded region growing, namely assigning the optimal coordinates of seeds, determining similarity differences, and evaluating segmentation quality. At this point, cluster validity index S_Dbw is used as two distinct objectives: scattering and density instead of its aggregating nature. So, maximum compactness for intra-region and minimum separation for inter-regions which are two conflicting objectives in image segmentation can be considered separately at the same time. Then SRG is executed in each objective evaluation for grouping pixels. Finally, the obtained segmentation takes its final form by post-processing operation which assigns all unlabeled pixels to a region. The algorithm is applied on test images obtained from BSDS and the outcomes are assessed by three region-based consistency measures which are called as LCE, GCE and BCE. Furthermore, the proposed method is compared with three accomplished algorithms. These are non-dominated sorting genetic algorithm II (NSGA2), non-dominated sorting particle swarm optimization (NSPSO) and fuzzy c-means (FCM). The experimental results show that the proposed method achieves high accuracy for image segmentation and it also has the best uniform distribution for multiple runnings. Consequently, it can be reported that the adapted version of IBMO is a well-designed and promising method for image segmentation.

Acknowledgement

Selcuk University Scientific Research Coordination (BAP) is acknowledged for its contribution to the financial support of this work.

Appendix A. Supplementary data

Supplementary data associated with this article can be found, in the online version, at http://dx.doi.org/10.1016/j.asoc.2015.05.016

References

[1] R.C. Gonzalez, R.E. Woods, Digital Image Processing, second ed., Prentice Hall, Upper Saddle River, NJ, 2002.

[2] E. Littmann, H. Ritter, Adaptive color segmentation – a comparison of neural and statistical methods, IEEE Trans. Neural Netw. 8 (1) (1997) 175–185.

[3] R.M. Haralick, L.G. Shapiro, Image segmentation techniques, Comput. Vis. Graph. Image Process. 29 (1) (1985) 100–132.

[4] P. Andrey, P. Tarroux, Unsupervised image segmentation using a distributed genetic algorithm, Pattern Recognit. 33 (5) (1993) 659–673.

[5] C. Cariou, K. Chehdi, Unsupervised texture segmentation/classification using 2-D autoregressive modeling and the stochastic expectation-maximization algorithm, Pattern Recognit. Lett. 29 (7) (2008) 905–917.

[6] M.G.H. Omran, A. Salman, A.P. Engelbrecht, Dynamic clustering using particle swarm optimization with application in image segmentation, Pattern Anal. Appl. 8 (1) (2005) 332–344.

[7] V. Ramos, F. Almeida, Artificial ant colonies in digital image habitats – a mass behavior effect study on pattern recognition, in: Proceedings of ANTS'2000 – 2nd International Workshop on Ant Algorithms, 2000, pp. 113–116.

[8] P. Huang, H. Cao, S. Luo, An artificial ant colonies approach to medical image segmentation, Comput. Methods Progr. Biomed. 92 (1) (2008) 267–273.

[9] M. Ma, J. Liang, M. Guo, Y. Fan, Y. Yin, SAR image segmentation based on artificial bee colony algorithm, Appl. Soft Comput. 11 (8) (2011) 5205–5214.

[10] M.G. Cinsdikici, D.A. Aydın, Detection of blood vessels in ophthalmoscope images using MF/ant (matched filter/ant colony) algorithm, Comput. Methods Progr. Biomed. 96 (2) (2009) 85–95.

[11] D. Aydın, A. Uğur, Extraction of flower regions in color images using ant colony optimization, Proc. Comput. Sci. 3 (1) (2011) 530–536.

[12] B. Akay, A study on particle swarm optimization and artificial bee colony algorithms for multilevel thresholding, Appl. Soft Comput. 13 (1) (2013) 3066–3091.

[13] T. Sağ, M. Çunkaş, Development of image segmentation techniques using swarm intelligence ABC-based clustering algorithm for image segmentation, in: International Conference on Computing and Information Technology, 2012, pp. 95–100.

[14] K.R. Mahmoud, M. El-Adawy, S.M.M. Ibrahem, A comparison between circular and hexagonal array geometries for smart antenna systems using particle swarm optimization algorithm, Prog. Electromagn. Res. 72 (1) (2007) 75–90.

[15] T. Sağ, M. Çunkaş, A tool for multiobjective evolutionary algorithms, Adv. Eng. Softw. 40 (9) (2009) 902–912.

[16] A. Nakib, H. Oulhadj, P. Siarry, Image thresholding based on Pareto multiobjective optimization, Eng. Appl. Artif. Intell. 23 (3) (2010) 313–320.

[17] S. Saha, S. Bandyopadhyay, Automatic MR brain image segmentation using a multiseed based multiobjective clustering approach, Appl. Intell. 35 (3) (2010) 411–427.

[18] I. Saha, U. Maulik, D. Plewczynski, A new multi-objective technique for differential fuzzy clustering, Appl. Soft Comput. 11 (2) (2011) 2765–2776.

[19] C.-W. Bong, M. Rajeshwari, Multi-objective nature-inspired clustering and classification techniques for image segmentation, Appl. Soft Comput. 11 (4) (2011) 3271–3282.

[20] T. Sağ, M. Çunkaş, A new ABC-based multi-objective optimization algorithm with an improvement approach (IBMO: improved bee colony algorithm for multi-objective optimization), Turk. J. Electr. Eng. Comput. Sci. (2014).

[21] T. Sağ, M. Cunkas, Application of multi-objective particle swarm optimization algorithm in image segmentation, in: 3rd World Conference on Information Technology (WCIT-2012), vol. 3, Glob. J. Technol. (2013).

[22] K. Deb, A. Pratap, S. Agarwal, T. Meyarivan, A fast and elitist multiobjective genetic algorithm: NSGA-II, IEEE Trans. Evol. Comput. 6 (1) (2002) 182–197.

[23] J.C. Bezdek, Pattern Recognition with Fuzzy Objective Function Algorithms, 1981, ISBN: 0-306-40671-3.

[24] S. Shirakawa, T. Nagao, Evolutionary image segmentation based on multiobjective clustering, in: Congress on Evolutionary Computation (CEC'09), Trondheim, Norway, 2009, pp. 2466–2473.

[25] C.A.C. Coello, A comprehensive survey of evolutionary-based multiobjective optimization techniques, Knowl. Inf. Syst. 1 (3) (1998) 129–156.

[26] D. Karaboga, An Idea Based on Honey Bee Swarm for Numerical Optimization. Technical Report, Erciyes University, Engineering Faculty, Computer Engineering Department, 2005.

[27] L. Busin, N. Vandenbroucke, L. Macaire, Color spaces and image segmentation, Adv. Imaging Electron Phys. 151 (1) (2008) 65–168.

[28] J.G. Daugman, Uncertainty relations for resolution in space, spatial frequency, and orientation optimized by two-dimensional visual cortical filters, J. Opt. Soc. Am. A 2 (1) (1985) 1160–1169.

[29] J.F. Khan, R.R. Adhami, S.M.A. Bhuiyan, A customized Gabor filter for unsupervised color image segmentation, Image Vis. Comput. 27 (2009) 489–501.

[30] D. Clausi, M. Ed Jernigan, Designing Gabor filters for optimal texture separability, Pattern Recognit. 33 (1) (2000) 1835–1849.

[31] H.D. Chengand, Y. Sun, A hierarchical approach to color image segmentation using homogeneity, IEEE Trans. Image Process. 9 (12) (2000) 2071–2082.

[32] R. Adams, L. Bischof, Seeded region growing, IEEE Trans. Pattern Anal. Mach. Intell. 16 (1) (1994) 641–647.

[33] O. Arbelaitz, I. Gurrutxaga, J. Muguerza, J.M. Prez, I. Perona, An extensive comparative study of cluster validity indices, Pattern Recognit. 46 (1) (2013) 243–256.

[34] U. Maulik, S. Bandyopadhyay, Performance evaluation of some clustering algorithms and validity indices, IEEE Trans. Pattern Anal. Mach. Intell. 24 (12) (2002) 1650–1654.

[35] M. Halkidi, Clustering Validity Assessment: Finding the Optimal Partitioning of a Data Set, 2001, pp. 187–194.

[36] D. Martin, C. Fowlkes, D. Tal, J. Malik, A database of human segmented natural images and its application to evaluating segmentation algorithms and measuring ecological statistics, in: Proceedings of the 8th International Conference on Computer Vision, vol. 2, No. 1, 2001, pp. 416–423.

[37] X.Y. Wang, T. Wang, J. Bu, Color image segmentation using pixel wise support vector machine classification, Pattern Recognit. 44 (2011) 777–787.